DFG-Schwerpunktprogramm 1324

„Extraktion quantifizierbarer Information aus komplexen Systemen”

Wavelet shrinkage on paths for scattered data denoising

D. Heinen, G. Plonka

Preprint 118

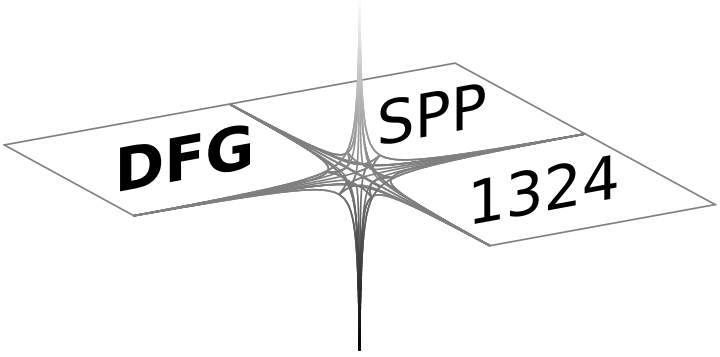

Edited by

AG Numerik/Optimierung
Fachbereich 12 - Mathematik und Informatik
Philipps-Universität Marburg
Hans-Meerwein-Str.
35032 Marburg

DFG-Schwerpunktprogramm 1324

„Extraktion quantifizierbarer Information aus komplexen Systemen”

Wavelet shrinkage on paths for scattered data denoising

D. Heinen, G. Plonka

Preprint 118

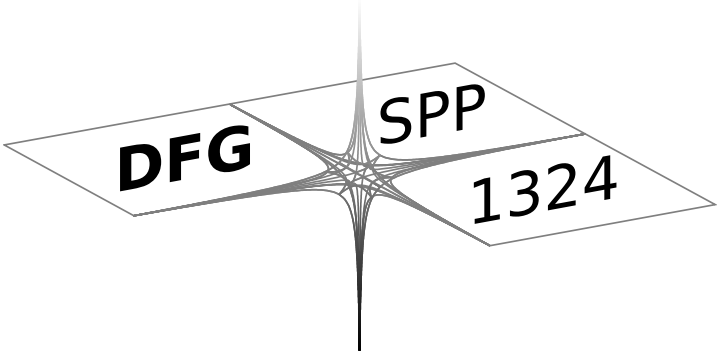

The consecutive numbering of the publications is determined by their chronological order.

The aim of this preprint series is to make new research rapidly available for scientific discussion. Therefore, the responsibility for the contents is solely due to the authors. The publications will be distributed by the authors.

Wavelet shrinkage on paths for scattered data denoising

Dennis Heinen and Gerlind Plonka

Dedicated to Werner Haußmann in memoriam

Abstract. We propose a new algorithm for denoising of multivariate function values given at scattered points in $\mathbb{R}^d$. The method is based on the one-dimensional wavelet transform that is applied along suitably chosen path vectors at each transform level. The idea can be seen as a generalization of the relaxed easy path wavelet transform in [13] to the case of multivariate scattered data. The choice of the path vectors is crucial for the success of the algorithm. We propose two adaptive path constructions that take the distribution of the scattered points as well as the corresponding function values into account. Further, we present some theoretical results on the wavelet transform along path vectors in order to indicate that the wavelet shrinkage along path vectors can really remove noise. The numerical results show the efficiency of the proposed denoising method.

Mathematics Subject Classification (2000). Primary42C40, 65T60; Secondary 68U10.

Keywords. scattered data denoising, wavelet shrinkage, path vectors, easy path wavelet transform.

1. Introduction

Within the last years, wavelet threshold methods have been shown to be a suitable tool for denoising of functions and images. In particular, using a translation-invariant filter bank, the visual artifacts in the neighborhood of discontinuities are well supressed [6]. The basic idea of wavelet denoising methods is a suitable separation of frequencies of a given noisy signal f. Supposing that the noise corresponds to wavelet coefficients with a small amplitude, the application of a thresholding procedure to the wavelet expansion of f removes it form the signal. Compared to other approaches to

This work has been supported by the German Research Foundation, grant PL 170/13-2.

image/signal denoising (as nonlinear diffusion or variational methods), one advantage of the wavelet denoising method is its numerical efficiency.

However, the traditional (tensor-product) wavelet transform only applies for equidistant grids. There have been several attempts to generalize the wavelet transform to functions that are sampled on non-equidistant or scattered points. In the one-dimensional case, some of these methods apply a certain approximation in a first step in order to get back the equidistant design situation [1, 3, 10, 12]. Other approaches that particularly apply in two or higher dimensions are based on the construction of second generation wavelets [17] by the lifting scheme, see e.g. [2, 7, 11, 19]. These wavelet constructions adaptively depend on the scattered points and the corresponding function values and therefore loose much of the simplicity and efficiency of the traditional wavelet transform.

In [13], the easy path wavelet transform (EPWT) has been introduced by one of the authors for sparse image approximation. The EPWT employs the one-dimensional wavelet transform along path vectors through the image values. The path vectors contain all indices (i, j) corresponding to the image values $f(i, j)$ and are determined in a way such that neighboring indices in the path are also neighboring in the two-dimensional grid and that the corresponding image values are well correlated. Obviously, the EPWT can be simply transferred to the setting of scattered data $x_j \in \mathbb{R}^d$ with corresponding function values $f(x_j) \in \mathbb{R}$, where we have just to generalize the notion of a neighborhood for x_j. A similar idea has been already applied in [14] for data on the sphere. The recently proposed generalized tree-based wavelet transform (GTBWT) [16] is closely related to the EPWT [13] and generalizes the Haar-like transform in [9]. In particular, the tree-based wavelet transform has been combined with a suitable sub-image averaging scheme for image denoising.

In this paper, we want to propose a new adaptive wavelet threshold scheme for scattered data denoising. The basic idea of our scheme is very similar to the EPWT, namely to employ the usual one-dimensional wavelet transform along suitable path vectors at each level. But we need to determine the path vectors differently in order to obtain good denoising results. Further, for resembling the cycle spinning method [6], we apply the wavelet threshold scheme several times along different path vectors and compute the average of the results.

The paper is organized as follows. In Section 2 we describe the general denoising algorithm along given path vectors. In Section 3 we propose two different methods for determining the path vectors, a deterministic and a random path construction. The two methods are both adaptive; the choice of the next path component adaptively depends on the spatial distance of the involved points x_j and the distance of the involved function values $f(x_j)$ (resp. the low pass values at further levels of the wavelet transform). In Section 4, we explore some theoretical results that support our approach for scattered data denoising. Finally, in Section 5 we present numerical results

of our data denoising method in the two-dimensional case. For the special case of images we also present some comparisons with other image denoising methods.

2. Description of the algorithm

Let $\Gamma = \{x_1, \ldots, x_N\}$ be the data set with scattered data points $x_j \in \mathbb{R}^d$, and let $f : \mathbb{R}^d \mapsto \mathbb{R}$ be a function sampled on $\Gamma \subset \Omega$, where Ω is a connected subset of $\mathbb{R}^d$ consisting of a finite union of convex domains. This means, the measured values $\tilde{f}(x_j)$ are given, where we assume that

$$\tilde{f}(x_j) = f(x_j) + z_j,$$

and z_j denotes additive Gaussian noise with zero mean and an (unknown) variance σ^2. For the distribution of the scattered data set Γ, we suppose quasi-uniformity, i.e., considering the maximal density

$$\delta(\Gamma) := \max_{x \in \Omega} \min_{k=1,\ldots,N} |x - x_k|$$

and the minimal spacing

$$\mu(\Gamma) := \min_{\substack{x_j, x_k \in \Gamma \\ j \neq k}} |x_j - x_k|,$$

we assume that $\delta(\Gamma) < C \cdot \mu(\Gamma)$, with a constant C independent of Ω and Γ. Further, we suppose that f is a piecewise smooth function.

Now, the basic idea of the new algorithm is the application of the classical wavelet shrinkage procedure along one-dimensional path vectors thereby generalizing the easy path wavelet transform (EPWT), see [13].

The EPWT was introduced for image approximation. Therefore, the path construction used in [13] is based on the strong correlation of function values corresponding to neighboring points in the path vector. A new point in the path vector is taken from the set of neighbor points, such that the difference of the corresponding function values is minimal. In case of noisy data, this approach for the path vector construction needs to be changed since the correlation of function values is now influenced by noise. In our algorithm, the construction of suitable path vectors turns out to be crucial for a good denoising performance.

Similarly to [9] and [16], we resemble the "cycle spinning" method [6] in order to improve the denoising procedure. For image denoising, it is usual to apply the tensor product wavelet shrinkage procedure not only to the noisy image itself but also to all images obtained by up to 7 cyclic shifts in x- and in y-direction. After application of the wavelet transform to each of the 64 images obtained in this way, an averaging is applied that greatly improves the denoising result. In our approach, we will just apply the path wavelet shrinkage procedure repeatedly along different path vectors and then average the result.

We summarize the complete algorithm before describing the path construction in more detail.

Algorithm 2.1.

Given: point set $\Gamma = \{x_1, \dots, x_N\} = \{x_1^0, \dots, x_N^0\} = \Gamma^0 \subset \mathbb{R}^d$,
$c_j^0 := \tilde{f}(x_j) = f(x_j) + z_j, \quad j = 1, \dots, N, \quad N = 2^t$,
biorthogonal wavelet filterbank with decomposition filters $\tilde{h}, \tilde{g}$ and reconstruction filters h, g

Iteration: Perform the following 4 steps for $l = 1, 2, \dots, L$ with $L < t$:

1. Find a suitable path vector $p^l \in \mathbb{R}^{N/2^l}$ consisting of a permutation of $\{1, \dots, N/2^l\}$ that describes a fixed order of points $x^l_{p^l(j)}$ and of the corresponding function values $c^l_{p^l(j)}$.
2. Apply the (periodic) low-pass filter $\tilde{h}$ to $(c^l_{p^l(j)})_{j=1}^N$ followed by downsampling by two to obtain the low-pass data $(c_j^{l+1})_{j=1}^{N/2^{l+1}}$. Apply the (periodic) high-pass filter $\tilde{g}$ to $(c^l_{p^l(j)})_{j=1}^N$ followed by downsampling by two to obtain the vector of wavelet coefficients $(d_j^{l+1})_{j=1}^{N/2^{l+1}}$.
3. Apply the normalized low-pass filter $\frac{1}{\sqrt{2}}\tilde{h}$ (such that $\frac{1}{\sqrt{2}} \sum_{l \in \mathbb{Z}} \tilde{h}_l = 1$) to the point vector $(x^l_{p^l(j)})_{j=1}^{N/2^l}$ (i.e., separately to all d components), followed by downsampling by two to obtain a new vector of scattered points $(x_j^{l+1})_{j=1}^{N/2^{l+1}}$.
   Determine the new point set $\Gamma^{l+1} := \{x_1^{l+1}, \dots, x^{l+1}_{N/2^{l+1}}\}$.
4. Apply a threshold procedure to the wavelet coefficients $(d_j^{l+1})_{j=1}^{N/2^{l+1}}$ to find
$$\tilde{d}_j^l = T_\theta(d_j^l) = \begin{cases} d_j^l & \text{if } |d_j^l| \geq \theta, \\ 0 & \text{if } |d_j^l| < \theta \end{cases}$$
   with a predefined threshold parameter $\theta > 0$.

Reconstruct the values $f(x_j)$ by the following iteration, where $(\tilde{c}_j^L)_{j=1}^{N/2^L} := (c_j^L)_{j=1}^{N/2^L}$.
Iteration: Perform the following three steps for $l = L, L-1, \dots, 1$:

5. Apply an upsampling by two first and then the low-pass filter h to $(\tilde{c}_j^l)_{j=1}^{N/2^l}$.
6. Apply an upsampling by two first and then the high-pass filter g to $(\tilde{d}_j^l)_{j=1}^{N/2^l}$.
7. Add the results of the previous two steps to obtain $(\tilde{c}^{l-1}_{p^{l-1}(j)})_{j=1}^{N/2^{l-1}}$ and apply the reverse permutation to get $(\tilde{c}_j^{l-1})_{j=1}^{N/2^{l-1}}$.

Output: $(\tilde{c}_j^0)_{j=1}^N$ the smoothed function values at scattered points $x_j \in \Gamma$.

As already remarked before, analogously to the cycle spinning approach, we apply the above algorithm several times and average the results in order to improve the denoising method.

Remark 2.2.
1. Observe that, similarly as for the EPWT in [13], the considered algorithm is usually not just a one-dimensional transform since the path vectors change at each level of the wavelet transform. This point is crucial for the performance of the denoising method. In particular, the set of scattered data points related to the computed low-pass values changes at each level according to step 3 of the algorithm. For a one-dimensional wavelet transform at equidistant points x_j on a line, step 3 of the algorithm just transforms the point set again into a (scaled) equidistant point set of half length on the line and needs therefore not to be considered.
2. In our numerical experiments for bivariate data, we have also obtained satisfying results by omitting step 3 of Algorithm 2.1 and by relating the low-pass data $(c_j^l)_{j=1}^{N/2^l}$ to a suitable subset of Γ. Here we take $\Gamma^1 := \{x_j^1 := x^0_{p^1(2j-1)} : j = 1, \ldots, N/2\} \subset \Gamma$, and generally

$$\Gamma^{l+1} := \{x_j^{l+1} := x^l_{p^{l+1}(2j-1)} : j = 1, \ldots, N/2^{l+1}\} \subset \Gamma.$$

3. It is possible to apply other shrinkage functions in step 4 of the algorithm as e.g. a firm shrinkage [8].

3. Construction of path vectors

The main challenge in the above denoising algorithm is to construct path vectors through the point sets Γ^l. As we will see in the sequel, the choice of the path vectors is crucial for the success of the denoising algorithm. For the path construction, we have to answer the following questions:

- How one needs to determine the neighborhood of scattered points as a tool for determination of the path vectors?
- How one needs to determine the distance between scattered points and between the corresponding function values? How we have to weight the distance $\|x_j^l - x_k^l\|_2$ and the difference of corresponding function/low-pass values $|c_j^l - c_k^l|$?
- Should the path vectors be chosen in a deterministic way or randomly, based on the point sets Γ^l and the corresponding data c_j^l?

In the remainder of this section, we shall propose two path vector constructions that we will use in our numerical examples.

3.1. Adaptive deterministic path construction

In $\mathbb{R}^d$, let us apply a neighborhood definition of the form

$$N(x_j^l) = \{x_k^l \in \Gamma^l : \|x_j^l - x_k^l\|_2 \leq 2^{l/d} \cdot C_1, j \neq k\}, \tag{3.1}$$

where C_1 depends on the distribution of the original point set Γ. Observe that the path vector at level l of the wavelet transform is a permutation of the indices of the points $\{x_j^l : j = 1, \ldots, N/2^l\}$. In particular, each point has

to occur exactly once in the path vector. In our numerical examples for $d = 2$, we take C_1 such that $N(x_j^0)$ with $x_j^0 := x_j \in \Gamma$ contains at least 8 entries for each $j \in \{1, \dots, N\}$. The path vectors at the level l of the wavelet transform are determined by the following procedure.

Algorithm 3.1. (Deterministic path construction)

Given: point set $\Gamma^l = \{x_1^l, \dots, x_{N/2^l}^l\} \subset \mathbb{R}^d$,
low pass values $c_j^l, \quad j = 1, \dots, N/2^l, \quad N = 2^t$.

Choose the first path component $p^l(1)$ randomly from $\{1, \dots, N/2^l\}$.

Iteration: Perform the following steps for $k = 1, \dots, N/2^l - 1$:

1. For a fixed shrinkage parameter θ, compute the subset

   $$N_\theta(x^l_{p^l(k)}) \subset \tilde{N}(x^l_{p^l(k)}) := \{x_r^l \in N(x^l_{p^l(k)}) : r \notin \{p^l(1), \dots, p^l(k)\}\}$$

   of points that have not been used in the path vector yet and whose corresponding function/low-pass values differ at most by θ, i.e.,

   $$N_\theta(x^l_{p^l(k)}) := \{x_r^l \in \tilde{N}(x^l_{p^l(k)}) : |c^l_{p^l(k)} - c_r^l| \le \theta\}. \tag{3.2}$$

2. Choose the next component in the path vector as follows.
   - If $N_\theta(x^l_{p^l(k)})$ is not empty, then choose the next path component $p^l(k+1)$ such that

   $$x^l_{p^l(k+1)} = \operatorname*{argmin}_{x \in N_\theta(x^l_{p^l(k)})} \left(\|x^l_{p^l(k)} - x^l_{p^l(k-1)}\|_2 - \|x^l_{p^l(k)} - x\|_2 \right), \tag{3.3}$$

   where we put $\|x^l_{p^l(1)} - x^l_{p^l(0)}\|_2 := 0$ for $k = 1$. For $k > 1$, you may alternatively choose $p^l(k+1)$ such that

   $$x^l_{p^l(k+1)} = \operatorname*{argmax}_{x \in N_\theta(x^l_{p^l(k)})} \frac{\langle x_{p^l(k-1)} - x_{p^l(k)}, x_{p^l(k)} - x \rangle}{\|x_{p^l(k-1)} - x_{p^l(k)}\| \cdot \|x_{p^l(k)} - x\|}. \tag{3.4}$$

   - If $N_\theta(x^l_{p^l(k)})$ is the empty set, we randomly choose the next path component from $\tilde{N}(x^l_{p^l(k)})$.
     If $\tilde{N}(x^l_{p^l(k)})$ is also empty, we choose the next index in the path vector randomly from the remaining indices of the point set

     $$\tilde{N}_{k,l} := \{x_r^l : r \notin \{p^l(1), \dots, p^l(k)\}\},$$

     or, if possible, from the subset

     $$\tilde{N}_{k,l,\theta} := \{x_r^l \in \tilde{N}_{k,l} : |c^l_{p^l(k)} - c_r^l| \le \theta\} \subset \tilde{N}_{k,l}.$$

Output: path vector $p^l = (p^l(k))_{k=1}^{N/2^l}$.

Remark 3.2.
The parameter θ that has to be chosen for determining the neighborhood $N_\theta(x^l_{p^l(k)})$ can be taken of the same size as the thresholding parameter for the wavelet transform in Algorithm 2.1.

Determining the $p^l(k+1)$ by (3.3) forces that scattered points corresponding to neighboring components in the path have similar distance, while (3.4) ensures the path to be continued in a similar direction as before, i.e., the angle between $x_{p^l(k-1)} - x_{p^l(k)}$ and $x_{p^l(k)} - x^l_{p^l(k+1)}$ is as small as possible. Theoretically, these requirements are supported by the fact that the polynomial reproduction property of low-pass filters (and the vanishing moment property of wavelet filters) can be exploited best for equidistantly sampled functions on a line, see Section 4. Of course, the two conditions (3.3) and (3.4) can also be coupled.

3.2. Adaptive random path construction

Instead of the adaptive path construction considered above, we may also apply a procedure, where the next path component is taken randomly from the remaining indices, and where the probability to choose the next index depends on the spatial distance of points on the one hand and on the distance of the corresponding function values on the other hand.

For the path construction at the l-th level, we now consider the vectors $y^l_j = ((x^l_j)^T, c^l_j)^T \in \mathbb{R}^{d+1}$ (with $c^0_j := \tilde{f}(x^0_j) = \tilde{f}(x_j)$) and define a symmetric weight matrix $W^l = (w(y^l_i, y^l_j))_{i,j=1}^{N/2^l}$, where the weights in the product

$$w(y^l_i, y^l_j) = w_1(x^l_i, x^l_j) \cdot w_2(c^l_i, c^l_j)$$

may be chosen differently, depending on the range of scattered points x^l_i and of the given (noisy) function values resp. low pass values c^l_i. A possible weight function, also used in the context of bilateral filtering [18], is

$$w(y^l_i, y^l_j) = \exp\left(\frac{-\|x^l_i - x^l_j\|_2^2}{2^{2l/d}\sigma_1}\right) \cdot \exp\left(\frac{-|c^l_i - c^l_j|^2}{2^l \sigma_2}\right) \tag{3.5}$$

where σ_1 and σ_2 need to be chosen appropriately. The normalization by $2^{2l/d}$ in the definition of the weight is due to the fact that each level of the wavelet transform involves a decimation of the number of scattered points by two, and the remaining points have a larger distances of each other. Regarding the low pass values, the range of these values grows by $\sqrt{2}$ due to the filter normalization $\sum_{l\in\mathbb{Z}} \tilde{h}_l = \sqrt{2}$.

While the proposed weight in (3.5) leads to a huge fully occupied weight matrix, we can strongly reduce the numerical effort by cutting the spatial weight at a suitable distance, i.e.

$$w_1(x^l_i, x^l_j) = \begin{cases} \exp(-\|x^l_i - x^l_j\|_2^2/(2^{2l/d}\sigma_1) & \|x^l_i - x^l_j\|_2 \le 2^{l/d} D_1, \\ 0 & \|x^l_i - x^l_j\|_2 > 2^{l/d} D_1, \end{cases}$$

where we have to choose D_1 appropriately to ensure a sufficiently large neighborhood for each point x^l_i. Similarly, the weight $w^l_2(c^l_i, c^l_j)$ may be just put to zero if the distance $|c^l_i - c^l_j|$ is greater than $2^{l/2} D_2$ with a suitable constant D_2. We propose now the following algorithm.

Algorithm 3.3. (Random path construction)

Given: point set $\Gamma^l = \{x_1^l, \dots, x_{N/2^l}^l\} \subset \mathbb{R}^d$, set of vectors $y_j^l = ((x_j^l)^T, c_j^l)^T$, low pass values $c_j^l, \quad j = 1, \dots, N/2^l, \quad N = 2^t$.

1. Compute the weight matrix $W^l = (w(y_i^l, y_j^l))_{i,j=1}^{N/2^l}$.
2. Choose the first path component $p^l(1)$ randomly from the index set $\{1, \dots, N/2^l\}$.
3. Considering the row $p^l(1)$ of the weight matrix W^l, let

$$s_{p^l(1)} := \sum_{\substack{j=1 \\ j \neq p^l(1)}}^{N/2^l} w(y_{p^l(1)}^l, y_j^l)$$

be the sum of weights in this row obtained by disregarding the diagonal element $w(y_{p^l(1)}^l, y_{p^l(1)}^l)$, and let now for $r \in \{1, \dots, N/2^l\} \setminus \{p^l(1)\}$,

$$P_{p^l(1),r} := \frac{w(y_{p^l(1)}^l, y_r^l)}{s_{p^l(1)}}$$

be the probability to choose r as the next component $p^l(2)$ in the path vector. Choose now $p^l(2)$ randomly from $\{1, \dots, N/2^l\} \setminus \{p^l(1)\}$ according to the determined probability distribution.

4. Generally, proceed with the following iteration for $k = 1, \dots, N/2^l - 1$. After having fixed the first k components $p^l(1), \dots, p^l(k)$ in the path vector, we consider the submatrix W_{k-1}^l obtained by deleting the $p^l(1)$-th,$\dots, p^l(k-1)$-th rows and columns of W^l, and apply the same procedure as before. We determine

$$s_{p^l(k)} = \sum_{\substack{j=1 \\ j \notin \{p^l(1), \dots, p^l(k)\}}}^{N/2^l} w(y_{p^l(k)}^l, y_j^l)$$

and compute the probability

$$P_{p^l(k),r} := \frac{w(y_{p^l(k)}^l, y_r^l)}{s_{p^l(k)}} \quad \text{for } r \in \{1, \dots, N/2^l\} \setminus \{p^l(1), \dots, p^l(k)\}.$$

Choose $p^l(k+1)$ randomly from $\{1, \dots, N/2^l\} \setminus \{p^l(1), \dots, p^l(k)\}$ according to the determined probability distribution.

Output: path vector $p^l = (p^l(k))_{k=1}^{N/2^l}$.

Remark 3.4.
1. For the two proposed path constructions, the choice of path vectors depends on the given (noisy) data values $c_j^0 = \tilde{f}(x_j)$ and the low-pass filtered values c_j^l and is hence adaptive. One may alternatively construct completely non-adaptive path vectors by taking into account only the neighborhoods of the given scattered points x_j^l at each level l (or only the spatial weights $w_1(x_i^l, x_j^l)$) and not the data values c_j^l. A non-adaptive denoising procedure possesses the advantage that all path vectors can be computed beforehand, such that a wavelet shrinkage procedure is similarly fast as a tensor product

wavelet shrinkage in the regular case. However, the results of the non-adaptive denoising approach are worse than the performance using the adaptively determined path vectors, see Section 5.
2. Our proposed adaptive path constructions significantly differ from the generalized tree constructions in [9] that depend only on the set of scattered points x_j and are hence non-adaptive.
3. The idea for determining the distribution for the random path vector construction is slightly related with the ideas for graph Laplacian constructions, see [5].

4. Properties of wavelet transform on paths

Usual wavelet filter banks possess a lot of favorable properties as polynomial reproduction of low-pass filters resp. vanishing moments of wavelet filters. For a given one-dimensional function f with a certain smoothness, a corresponding decay of wavelet coefficients $d_k^l(f)$ in the wavelet expansion

$$f(x) = \sum_{l,k} d_k^l(f)\psi_{l,k}(x)$$

can be shown. Within the last years, this property has been extensively exploited for function space characterizations by means of wavelet expansions. Conversely, wavelet coefficients of high magnitude indicate discontinuities (or points of lower smoothness). The success of wavelet denoising algorithms by thresholding of wavelet coefficients is based on these properties, since for (piecewise) smooth functions, small wavelet coefficients are related to noise. Considering now the case of scattered data $\{x_1, \dots, x_N\}$ in the multivariate case and the wavelet transform along certain path vectors, we may ask, whether the favorable properties of wavelet transform at least partially transfer to this setting. Regarding the polynomial reproduction of the low-pass filters along path vectors of scattered data, we find

Theorem 4.1. *Let $(\tilde{h}_k)_{k\in\mathbb{Z}}$ be the low-pass filter of the decomposition step in a wavelet filter bank of perfect reconstruction with $\sum_{k\in\mathbb{Z}} \tilde{h}_k = 1$. Further, let $p^1 = (p^1(j))_{j=1}^N$ be the path vector for ordering the scattered data points $x_j = (x_{j,1}, \dots, x_{j,d})^T \in \mathbb{R}^d$. Applying the low-pass filter $\tilde{h}$ to the sequence $(f(x_j))_{j=1}^N$, where $f(x) = a^T x + b$ is a d-variate linear polynomial with $a \in \mathbb{R}^d$, $b \in \mathbb{R}$, the sequence of low-pass coefficients $(c_j^1)_{j=1}^{N/2}$ obtained by one decomposition step of the wavelet filter bank along the path p^1 again reproduces f at the points $(x_j^1)_{j=1}^{N/2}$ with $x_j^1 = \sum_{k\in\mathbb{Z}} \tilde{h}_k x_{p^1(2j-1-k)}$, i.e., we have*

$$f(x_j^1) = c_j^1.$$

Proof. Application of the filter $(\tilde{h}_k)_{k\in\mathbb{Z}}$ to the sequence of function values along the path p^1 gives

$$(c_j^1)_{j=1}^{N/2} := (\sum_{k\in\mathbb{Z}} \tilde{h}_k f(x_{p^1(2j-1-k)}))_{j=1}^{N/2}$$

with

$$c_j^1 = \sum_{k\in\mathbb{Z}} \tilde{h}_k (a^T x_{p^1(2j-1-k)} + b) = a^T \Big(\sum_{k\in\mathbb{Z}} \tilde{h}_k x_{p^1(2j-1-k)}\Big) + b \sum_{k\in\mathbb{Z}} \tilde{h}_k.$$

Hence the assertion of the theorem follows using the new sequence of scattered points x_j^1 with

$$x_j^1 = \sum_{k\in\mathbb{Z}} \tilde{h}_k x_{p^1(2j-1-k)},$$

where $(x_j^1)_{l=1}^{N/2}$ is obtained by (componentwisely) applying the low-pass filter $\tilde{h}$ and downsampling to the sequence of scattered points $(x_{p^1(j)})_{j=1}^N$ ordered along the path p^1. □

We suppose that the wavelet filter $\tilde{g} = (\tilde{g}_k)_{k\in\mathbb{Z}}$ in the decomposition step of the wavelet filter bank satisfies the moment conditions $\sum_{k\in\mathbb{Z}} g_k = 0$ and $\sum_{k\in\mathbb{Z}} k g_k = 0$. Considering the wavelet coefficients obtained by applying the wavelet filter $\tilde{g}$ along the path vector p^1 followed by downsampling, we observe that a constant function $f(x) = c$, $c \in \mathbb{R}$, yields the wavelet coefficients

$$d_j^1 = \sum_{k\in\mathbb{Z}} \tilde{g}_k f(x_{p^1(2j-1-k)}) = c \cdot \sum_{k\in\mathbb{Z}} \tilde{g}_k = 0,$$

while for a linear polynomial $f(x) = a^T x + b$ with $a \in \mathbb{R}^d$ and $b \in \mathbb{R}$, the wavelet coefficients

$$d_j^1 = \sum_{k\in\mathbb{Z}} \tilde{g}_k (a^T x_{p^1(2j-1-k)} + b) = a^T \Big(\sum_{k\in\mathbb{Z}} \tilde{g}_k x_{p^1(2j-1-k)}\Big) + b \sum_{k\in\mathbb{Z}} g_k$$

can only vanish if the sequence $(x_{p^1(2j-1-k)})_{k\in\mathbb{Z}}$ is linear in each component. This observation implies that path vectors p^l should locally be chosen such that the values in the d component sequences $(x_{p^1(2j-1-k),\nu})_{k\in\mathbb{Z}}$, $\nu = 1, \ldots, d$, lie approximately equidistantly on a line if f is smooth in this region, see (3.3) and (3.4) in Algorithm 3.1.

Regarding the decay of wavelet coefficients obtained by a wavelet transform along paths (using a different path at each level), we can apply the results of [15] for two-dimensional piecewise Hölder continuous functions of order $\alpha \in (0, 1]$ thereby supporting our procedure of data denoising via wavelet transforms along paths.

Let $\{\Omega_i\}_{1\le i\le K}$ be a finite set of regions in $[0, 1)^2$ such that $\bigcup_{i=1}^K \Omega_i = [0, 1)^2$ and $\Omega_i \cap \Omega_j = \emptyset$ for $i \neq j$, and where $\overline{\Omega}_i$ is assumed to be a connected subset of $[0, 1]^2$ for each $i = 1, \ldots, K$. Further, let us assume that the bivariate function f satisfies a Hölder condition in each region $\Omega_i, 1 \le i \le K$, i.e.

$$|f(x) - f(x + h)| \le C\|h\|_2^\alpha \qquad \text{for } x, x + h \in \Omega_i$$

for some $\alpha \in (0, 1]$ and $C > 0$ independent of i. Let the function f be uniformly sampled on Ω, i.e., we have given $f(x_{j_1,j_2})$ with $x_{j_1,j_2} \in I_{2J} := \{(\frac{j_1}{2^J}, \frac{j_2}{2^J}),\ j_1, j_2 = 0, \ldots 2^J - 1\}$, and $N = 2^{2J}$. We can perform up to $L = 2J$ levels of the wavelet transform along path vectors (EPWT).

For such "cartoon-like" functions, it has been shown in [15] that the EPWT wavelet coefficients corresponding to one region Ω_i satisfy the estimate

$$|d_k^l(f)| \leq \frac{1}{2} C D^\alpha 2^{-(2J-l)(\alpha+1)/2},$$

where C is the Hölder constant and α the Hölder exponent. The constant D measures the uniformity of the scattered points after each level, where we assume that

$$\min |x_j^l - x_k^l| < D 2^{l/2}.$$

This condition is described as "diameter condition" in [15] and can be interpreted as a condition on the choice of the path vectors. Moreover, it has been shown in [15] that for $J \to \infty$, the EPWT leads to an asymptotically optimal N-term approximation f_N of f satisfying the estimate

$$\|f - f_N\|_{L^2(\Omega)}^2 \leq \tilde{C}\, N^{-\alpha},$$

where f_N is the two-dimensional function that is reconstructed from the N most significant EPWT-wavelet coefficients. The above optimal approximation result holds under the assumption that the path vectors p^l at each level of the EPWT transform satisfy (besides the diameter condition) a second condition, termed "region condition" [15]. The region condition ensures that the next index in the path vector p^l should be taken from the same region Ω_i if possible, before crossing to another region. The two conditions on the path vectors required in [15] are both contained in our algorithm. In the adaptive deterministic path construction, the neighborhood definition in (3.1) ensures the diameter condition while the neighborhood definition $N_\theta(x)$ in (3.2) provides the region condition. In the random path construction, the two path conditions are included by the choice of the weight that produces higher probabilities for those indices to be the next path component whose spatial distance $\|x^l_{p^l(k)} - x^l_{p^l(k+1)}\|_2$ as well as distance of function values/low pass values $|c^l_{p^l(k)} - c^l_{p^l(k+1)}|$ are small.

Hence the N-term approximation result in [15] can be taken as a further evidence, that small wavelet coefficients are rather due to noise than to important signal structure.

5. Numerical results

We want to apply the proposed scattered data wavelet denoising algorithm along path vectors to 256×256 pixel images. The noisy images in this subsection are generated by adding synthetic white Gaussian noise to the original natural images. The quality of the denoising results is measured by the peak signal to noise ratio (PSNR) given by

$$\text{PSNR} = 10 \log_{10} \frac{\max_{j=1,\ldots,N} f(x_j)}{\frac{1}{N}\sum_{j=1}^N (\tilde{f}(x_j) - f(x_j))^2},$$

where f denotes the original and $\tilde{f}$ the noisy image. In our experiments we have taken $\max_{j=1,\dots,N} f(x_j) = 255$.

In Figure 1, we present the original pepper image (a), the noisy pepper image (b) with PSNR = 19.97, and the denoising results using several different algorithms. In particular, we consider the 7-9 biorthogonal tensor-product wavelet shrinkage (c) with a PSNR of 24.91, the 7-9 biorthogonal wavelet shrinkage with cycle spinning (d) with 64 shifts and a PSNR of 28.11, the four-pixel scheme by Welk, Steidl and Weickert [20] (e) using 76 iterations and a step size $\tau = 0.001$ providing a PSNR of 28.26, and the curvelet shrinkage (e) with best threshold parameter 80 yielding a PSNR of 26.36. The curvelet denoising result is obtained with the help of the CurveLab software that is available at www.curvelet.org, see also [4]. The results of our algorithm (using a 7-9 biorthogonal wavelet filter bank) with a deterministic path vector (g) and a random path vector (h) are given in Figures 1(g) and 1(h). For the tensor-product wavelet shrinkage we have used the shrinkage parameter $\theta = 74$. For the deterministic path vector construction in (3.2) we have taken $C_1 = 1.3$ and shrinkage parameter $\theta = 89$. For the random path vectors that perform slightly worse than the deterministic vectors, we have taken the weight with $\sigma_1 = \sigma_2 = 0.2$, $D_1 = 5.0$ and $\theta = 71$. Further, we have 64 times applied Algorithm 2.1 and have averaged the results. The parameters for the curvelet transform and for the four-pixel scheme have been taken such that they perform optimally.

In Figure 2, we present the denoising results for the noisy pepper image with a PSNR of 16.45. Again, we compare our denoising results with tensor-product shrinkage, the four-pixel scheme and with curvelet shrinkage. For the tensor product case with the biorthogonal 7-9 filter bank we have used the optimal threshold $\theta = 140$ (without cycle spinning) and $\theta = 115$ (with cycle spinning). The four-pixel scheme works best with a time step of 0.001 and 124 iterations. The curvelet shrinkage uses the optimal thresholds $\theta = 106$. For our method with the deterministic path we have taken the threshold $\theta = 127$ and $C_1 = 1.1$; for the random path the same threshold and a weight with $\sigma_1 = \sigma_2 = 0.2$ and with $D_1 = 5$.

The denoising results for the pepper image and for the cameraman image of size 256×256 are summarized in Table 1, where we have chosen optimal parameters for each method.

In Figure 3, we illustrate the remaining scattered points obtained after different levels of our deterministic path algorithm that is applied to the cameraman image. The results show that the points are rather well distributed. These points are at a time used for constructing the next path vector.

Finally, we will show a denoising experiment, where we do not longer consider a rectangular region but a region with an L-form, see Figure 4. Here we have used deterministic path vectors with threshold $\theta = 89$ and with $C_1 = 1.3$. The main advantage of our new scattered data denoising algorithm is that we can apply it to denoise functions on any connected region, where

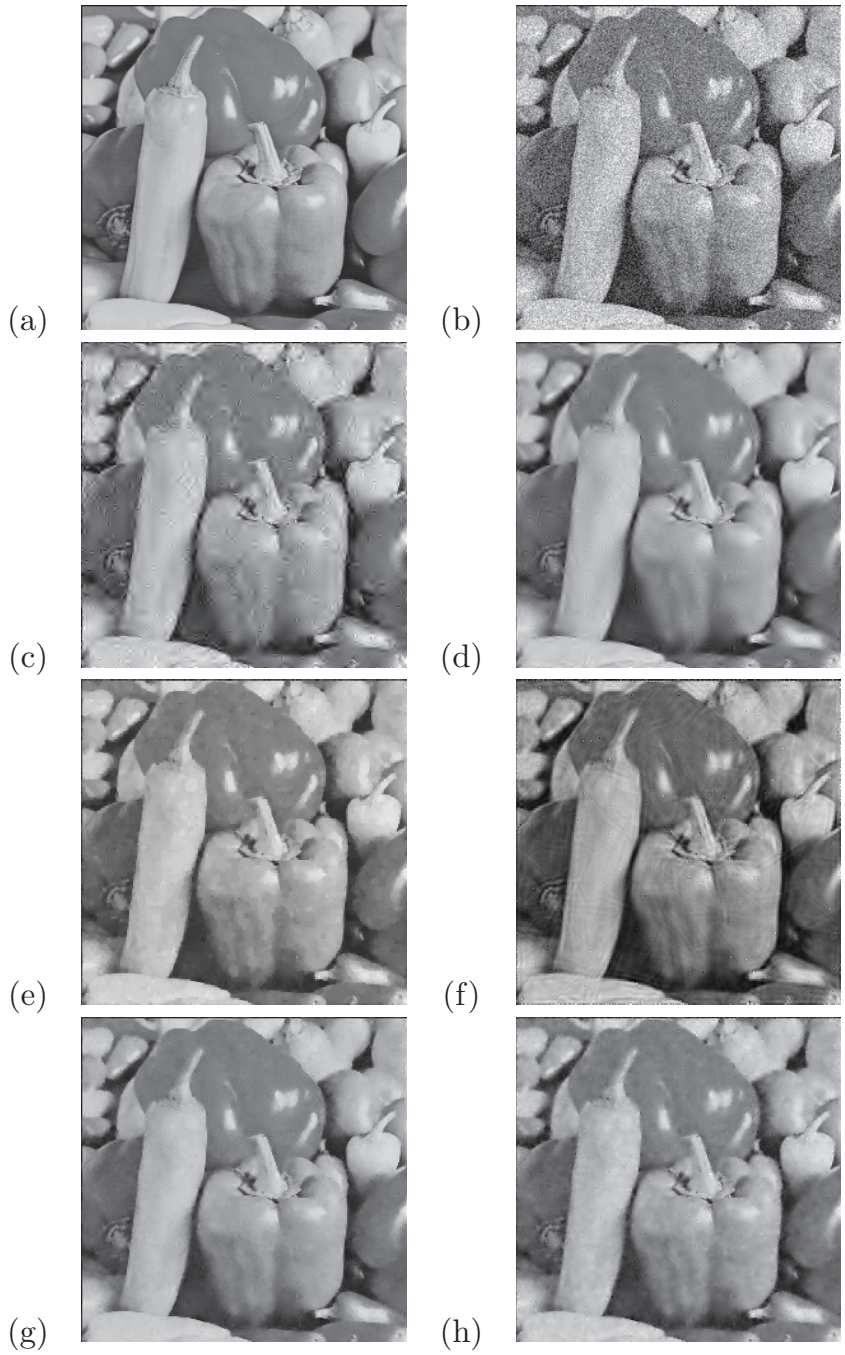

Figure 1. Top: (a) original image, (b) noisy image, PSNR 19.97; second row: denoising by tensor product biorthogonal 7-9 wavelet transform (c) without cycle spinning, PSNR 24.91; (d) with cycle spinning with 64 shifts, PSNR 28.11; third row: four pixel scheme, PSNR 28.26; (f) curvelet shrinkage, PSNR 26.36; last row: our scheme with (g) deterministic path, PSNR 29.01; (h) random path, PSNR 27.96.

we have to adjust step 3 of Algorithm 2.1 suitably as e.g. given in Remark 2.2.

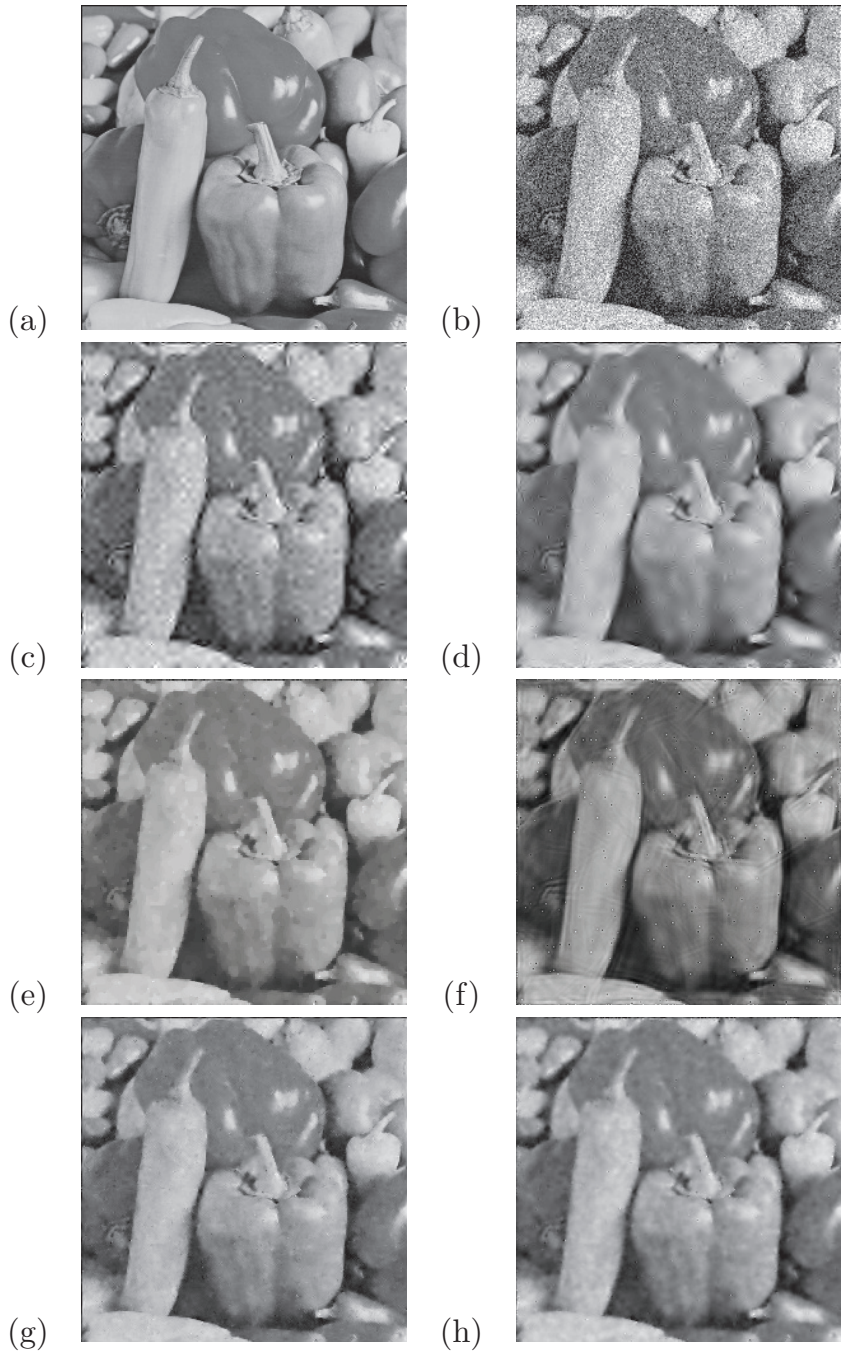

Figure 2. Top: (a) original image, (b) noisy image, PSNR 16.45; second row: denoising by tensor product biorthogonal 7-9 wavelet transform (c) without cycle spinning, PSNR 23.20; (d) with cycle spinning with 64 shifts, PSNR 25.86; third row: four pixel scheme, PSNR 26.13; (f) curvelet shrinkage, PSNR 23.95; last row: our scheme with (g) deterministic path, PSNR 26.44; (h) random path, PSNR 25.69.

Acknowledgment

This work is supported by the priority program SPP 1324 of the Deutsche Forschungsgemeinschaft (DFG), project PL 170/13-2.

image	noisy image	tensor 7-9	cycle 7-9	[20]	curvelet shrink.	determ. path	random path
pepper	19.97	24.91	28.11	28.26	26.36	**29.01**	27.96
pepper	16.45	23.20	25.86	26.13	23.95	**26.44**	25.69
cameraman	19.97	24.74	27.19	27.64	25.48	**28.28**	27.44
cameraman	16.45	22.86	25.14	25.73	23.73	**26.15**	24.85

Table 1. Comparison of our scattered data denoising method with deterministic and random path vectors with other denoising methods, see also Figures 1 and 2.

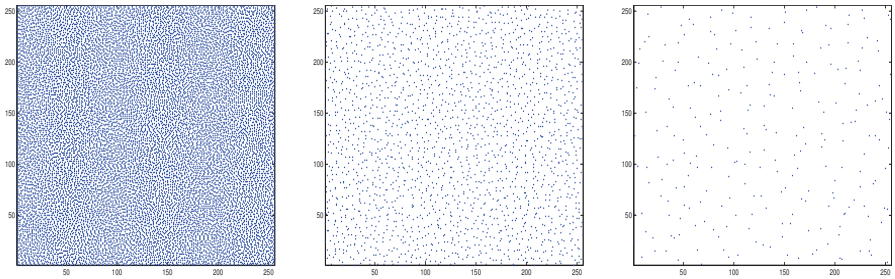

Figure 3. Scattered points after the second level (left), the fifth level (middle) and the eights level (right) of the denoising algorithm.

Figure 4. L-sector of the cameraman image, original (left), noisy image with PSNR of 19.97 (middle) and denoised image with the proposed method using a deterministic path vector with a PSNR of 27.77.

References

[1] A. Antoniadis and D.T. Pham, Wavelet regression for random or irregular design, *Comput. Statist. Data Anal.* **28** (1998), 353–369.

[2] R. Baraniuk, A. Cohen, and R. Wagner, Approximation and compression of scattered data by meshless multiscale decompositions, *Appl. Comput. Harmon. Anal.* **25** (2008), 133–147.

[3] T. Cai and L.D. Brown, Wavelet shrinkage for nonequispaced samples, *Ann. Statist.* **26**(5) (1998), 1783–1799.

[4] E. Candes, L. Demanet, D. Donoho, and L.Ying, Fast discrete curvelet transforms, *Multiscale Model. Simul.* **5** (2006), 861–899.

[5] F. Chung, Spectral Graph Theory, CBMS Regional Conference Series in Mathematics **92**, Amer. Math. Soc., Providence, RI, 1997.

[6] R.R. Coifman and D.L. Donoho, Translation-invariant de-noising, in *Wavelets and Statistics*, A. Antoniadis and G. Oppenheim, eds., Springer-Verlag, New York, 1995, pp. 125–150.

[7] V. Delouille, Nonparametric stochastic regression using design-adapted wavelets, Ph.D. Thesis, Universite Catholique de Louvain, 2002.

[8] H.-Y. Gao and A. G. Bruce, WaveShrink with firm shrinkage, *Statistica Sinica* **7** (1997), 855–874.

[9] M. Gavish, B. Nadler, and R.R. Coifman, Multiscale wavelets on trees, graphs and high-dimensional data: Theory and applications to semi supervised learning, *Proceedings of the 27th International Conference on Machine Learning*, 2010.

[10] P. Hall and B.A. Turlach, Interpolation methods for nonlinear wavelet regression with irregularly spaced design. *Ann. Statist.* **25**(5) (1997), 1912–1925.

[11] M. Jansen, G. Nason, and B. Silverman, Scattered data smoothing by empirical Bayesian shrinkage of second generation wavelet coefficients, Wavelet App. in Sig. and Image Processing IX, Proc. of SPIE. 4478 (2001), 87–97.

[12] A. Kovac and B.W. Silverman, Extending the scope of wavelet regression methods by coefficient-dependent thresholding. *J. A. Statist. Assoc.* **95** (2000), 172–183.

[13] G. Plonka, The easy path wavelet transform: a new adaptive wavelet transform for sparse representation of two-dimensional data, *Multiscale Model. Simul.* **7** (2009), 1474–1496.

[14] G. Plonka and D. Roşca, Easy path wavelet transform on triangulations of the sphere, *Mathematical Geosciences* **42**(7) (2010), 839–855.

[15] G. Plonka, S. Tenorth, and A. Iske, Optimally Sparse Image Representation by the Easy Path Wavelet Transform. *Int. J. Wavelets Multiresolut. Inf. Process.* (2012), to appear.

[16] I. Ram, M. Elad, and I. Cohen, Generalized tree-based wavelet transform, IEEE Trans. Signal Process. **59**(9) (2011), 4199–4209.

[17] W. Sweldens, The lifting scheme: A construction of second generation wavelets, *SIAM J. Math. Anal.* **29**(2) (1997), 511-546.

[18] C. Tomasi and R. Manduchi, Bilateral filtering for gray and color images, in *Proc. 6th Int. Conf. Computer Vision*, New Delhi, India, 1998, 839–846.

[19] E. Vanraes, M. Jansen, and A. Butheel, Stabilized wavelet transforms for non-equispaced data smoothing. *Signal Process.* **82**(12) (2002), 1979–1990.

[20] M. Welk, J. Weickert, and G. Steidl, A four-pixel scheme for singular differential equations. In: R. Kimmel, N. Sochen, J. Weickert (Eds.), *Scale-Space and PDE Methods in Computer Vision*, Lecture Notes in Computer Science 3459, Springer, Berlin (2005) 610–621.

Dennis Heinen
University of Göttingen
Institute for Numerical and Applied Mathematics
Lotzestr. 16-18
37083 Göttingen
Germany
e-mail: d.heinen@math.uni-goettingen.de

Gerlind Plonka
University of Göttingen
Institute for Numerical and Applied Mathematics
Lotzestr. 16-18
37083 Göttingen
Germany
e-mail: plonka@math.uni-goettingen.de

Preprint Series DFG-SPP 1324

http://www.dfg-spp1324.de

Reports

[1] R. Ramlau, G. Teschke, and M. Zhariy. A Compressive Landweber Iteration for Solving Ill-Posed Inverse Problems. Preprint 1, DFG-SPP 1324, September 2008.

[2] G. Plonka. The Easy Path Wavelet Transform: A New Adaptive Wavelet Transform for Sparse Representation of Two-dimensional Data. Preprint 2, DFG-SPP 1324, September 2008.

[3] E. Novak and H. Woźniakowski. Optimal Order of Convergence and (In-) Tractability of Multivariate Approximation of Smooth Functions. Preprint 3, DFG-SPP 1324, October 2008.

[4] M. Espig, L. Grasedyck, and W. Hackbusch. Black Box Low Tensor Rank Approximation Using Fibre-Crosses. Preprint 4, DFG-SPP 1324, October 2008.

[5] T. Bonesky, S. Dahlke, P. Maass, and T. Raasch. Adaptive Wavelet Methods and Sparsity Reconstruction for Inverse Heat Conduction Problems. Preprint 5, DFG-SPP 1324, January 2009.

[6] E. Novak and H. Woźniakowski. Approximation of Infinitely Differentiable Multivariate Functions Is Intractable. Preprint 6, DFG-SPP 1324, January 2009.

[7] J. Ma and G. Plonka. A Review of Curvelets and Recent Applications. Preprint 7, DFG-SPP 1324, February 2009.

[8] L. Denis, D. A. Lorenz, and D. Trede. Greedy Solution of Ill-Posed Problems: Error Bounds and Exact Inversion. Preprint 8, DFG-SPP 1324, April 2009.

[9] U. Friedrich. A Two Parameter Generalization of Lions' Nonoverlapping Domain Decomposition Method for Linear Elliptic PDEs. Preprint 9, DFG-SPP 1324, April 2009.

[10] K. Bredies and D. A. Lorenz. Minimization of Non-smooth, Non-convex Functionals by Iterative Thresholding. Preprint 10, DFG-SPP 1324, April 2009.

[11] K. Bredies and D. A. Lorenz. Regularization with Non-convex Separable Constraints. Preprint 11, DFG-SPP 1324, April 2009.

[12] M. Döhler, S. Kunis, and D. Potts. Nonequispaced Hyperbolic Cross Fast Fourier Transform. Preprint 12, DFG-SPP 1324, April 2009.

[13] C. Bender. Dual Pricing of Multi-Exercise Options under Volume Constraints. Preprint 13, DFG-SPP 1324, April 2009.

[14] T. Müller-Gronbach and K. Ritter. Variable Subspace Sampling and Multi-level Algorithms. Preprint 14, DFG-SPP 1324, May 2009.

[15] G. Plonka, S. Tenorth, and A. Iske. Optimally Sparse Image Representation by the Easy Path Wavelet Transform. Preprint 15, DFG-SPP 1324, May 2009.

[16] S. Dahlke, E. Novak, and W. Sickel. Optimal Approximation of Elliptic Problems by Linear and Nonlinear Mappings IV: Errors in L_2 and Other Norms. Preprint 16, DFG-SPP 1324, June 2009.

[17] B. Jin, T. Khan, P. Maass, and M. Pidcock. Function Spaces and Optimal Currents in Impedance Tomography. Preprint 17, DFG-SPP 1324, June 2009.

[18] G. Plonka and J. Ma. Curvelet-Wavelet Regularized Split Bregman Iteration for Compressed Sensing. Preprint 18, DFG-SPP 1324, June 2009.

[19] G. Teschke and C. Borries. Accelerated Projected Steepest Descent Method for Nonlinear Inverse Problems with Sparsity Constraints. Preprint 19, DFG-SPP 1324, July 2009.

[20] L. Grasedyck. Hierarchical Singular Value Decomposition of Tensors. Preprint 20, DFG-SPP 1324, July 2009.

[21] D. Rudolf. Error Bounds for Computing the Expectation by Markov Chain Monte Carlo. Preprint 21, DFG-SPP 1324, July 2009.

[22] M. Hansen and W. Sickel. Best m-term Approximation and Lizorkin-Triebel Spaces. Preprint 22, DFG-SPP 1324, August 2009.

[23] F.J. Hickernell, T. Müller-Gronbach, B. Niu, and K. Ritter. Multi-level Monte Carlo Algorithms for Infinite-dimensional Integration on $\mathbb{R}^{\mathbb{N}}$. Preprint 23, DFG-SPP 1324, August 2009.

[24] S. Dereich and F. Heidenreich. A Multilevel Monte Carlo Algorithm for Lévy Driven Stochastic Differential Equations. Preprint 24, DFG-SPP 1324, August 2009.

[25] S. Dahlke, M. Fornasier, and T. Raasch. Multilevel Preconditioning for Adaptive Sparse Optimization. Preprint 25, DFG-SPP 1324, August 2009.

[26] S. Dereich. Multilevel Monte Carlo Algorithms for Lévy-driven SDEs with Gaussian Correction. Preprint 26, DFG-SPP 1324, August 2009.

[27] G. Plonka, S. Tenorth, and D. Roşca. A New Hybrid Method for Image Approximation using the Easy Path Wavelet Transform. Preprint 27, DFG-SPP 1324, October 2009.

[28] O. Koch and C. Lubich. Dynamical Low-rank Approximation of Tensors. Preprint 28, DFG-SPP 1324, November 2009.

[29] E. Faou, V. Gradinaru, and C. Lubich. Computing Semi-classical Quantum Dynamics with Hagedorn Wavepackets. Preprint 29, DFG-SPP 1324, November 2009.

[30] D. Conte and C. Lubich. An Error Analysis of the Multi-configuration Time-dependent Hartree Method of Quantum Dynamics. Preprint 30, DFG-SPP 1324, November 2009.

[31] C. E. Powell and E. Ullmann. Preconditioning Stochastic Galerkin Saddle Point Problems. Preprint 31, DFG-SPP 1324, November 2009.

[32] O. G. Ernst and E. Ullmann. Stochastic Galerkin Matrices. Preprint 32, DFG-SPP 1324, November 2009.

[33] F. Lindner and R. L. Schilling. Weak Order for the Discretization of the Stochastic Heat Equation Driven by Impulsive Noise. Preprint 33, DFG-SPP 1324, November 2009.

[34] L. Kämmerer and S. Kunis. On the Stability of the Hyperbolic Cross Discrete Fourier Transform. Preprint 34, DFG-SPP 1324, December 2009.

[35] P. Cerejeiras, M. Ferreira, U. Kähler, and G. Teschke. Inversion of the noisy Radon transform on $SO(3)$ by Gabor frames and sparse recovery principles. Preprint 35, DFG-SPP 1324, January 2010.

[36] T. Jahnke and T. Udrescu. Solving Chemical Master Equations by Adaptive Wavelet Compression. Preprint 36, DFG-SPP 1324, January 2010.

[37] P. Kittipoom, G. Kutyniok, and W.-Q Lim. Irregular Shearlet Frames: Geometry and Approximation Properties. Preprint 37, DFG-SPP 1324, February 2010.

[38] G. Kutyniok and W.-Q Lim. Compactly Supported Shearlets are Optimally Sparse. Preprint 38, DFG-SPP 1324, February 2010.

[39] M. Hansen and W. Sickel. Best m-Term Approximation and Tensor Products of Sobolev and Besov Spaces – the Case of Non-compact Embeddings. Preprint 39, DFG-SPP 1324, March 2010.

[40] B. Niu, F.J. Hickernell, T. Müller-Gronbach, and K. Ritter. Deterministic Multi-level Algorithms for Infinite-dimensional Integration on $\mathbb{R}^{\mathbb{N}}$. Preprint 40, DFG-SPP 1324, March 2010.

[41] P. Kittipoom, G. Kutyniok, and W.-Q Lim. Construction of Compactly Supported Shearlet Frames. Preprint 41, DFG-SPP 1324, March 2010.

[42] C. Bender and J. Steiner. Error Criteria for Numerical Solutions of Backward SDEs. Preprint 42, DFG-SPP 1324, April 2010.

[43] L. Grasedyck. Polynomial Approximation in Hierarchical Tucker Format by Vector-Tensorization. Preprint 43, DFG-SPP 1324, April 2010.

[44] M. Hansen und W. Sickel. Best m-Term Approximation and Sobolev-Besov Spaces of Dominating Mixed Smoothness - the Case of Compact Embeddings. Preprint 44, DFG-SPP 1324, April 2010.

[45] P. Binev, W. Dahmen, and P. Lamby. Fast High-Dimensional Approximation with Sparse Occupancy Trees. Preprint 45, DFG-SPP 1324, May 2010.

[46] J. Ballani and L. Grasedyck. A Projection Method to Solve Linear Systems in Tensor Format. Preprint 46, DFG-SPP 1324, May 2010.

[47] P. Binev, A. Cohen, W. Dahmen, R. DeVore, G. Petrova, and P. Wojtaszczyk. Convergence Rates for Greedy Algorithms in Reduced Basis Methods. Preprint 47, DFG-SPP 1324, May 2010.

[48] S. Kestler and K. Urban. Adaptive Wavelet Methods on Unbounded Domains. Preprint 48, DFG-SPP 1324, June 2010.

[49] H. Yserentant. The Mixed Regularity of Electronic Wave Functions Multiplied by Explicit Correlation Factors. Preprint 49, DFG-SPP 1324, June 2010.

[50] H. Yserentant. On the Complexity of the Electronic Schrödinger Equation. Preprint 50, DFG-SPP 1324, June 2010.

[51] M. Guillemard and A. Iske. Curvature Analysis of Frequency Modulated Manifolds in Dimensionality Reduction. Preprint 51, DFG-SPP 1324, June 2010.

[52] E. Herrholz and G. Teschke. Compressive Sensing Principles and Iterative Sparse Recovery for Inverse and Ill-Posed Problems. Preprint 52, DFG-SPP 1324, July 2010.

[53] L. Kämmerer, S. Kunis, and D. Potts. Interpolation Lattices for Hyperbolic Cross Trigonometric Polynomials. Preprint 53, DFG-SPP 1324, July 2010.

[54] G. Kutyniok and W.-Q Lim. Shearlets on Bounded Domains. Preprint 54, DFG-SPP 1324, July 2010.

[55] A. Zeiser. Wavelet Approximation in Weighted Sobolev Spaces of Mixed Order with Applications to the Electronic Schrödinger Equation. Preprint 55, DFG-SPP 1324, July 2010.

[56] G. Kutyniok, J. Lemvig, and W.-Q Lim. Compactly Supported Shearlets. Preprint 56, DFG-SPP 1324, July 2010.

[57] A. Zeiser. On the Optimality of the Inexact Inverse Iteration Coupled with Adaptive Finite Element Methods. Preprint 57, DFG-SPP 1324, July 2010.

[58] S. Jokar. Sparse Recovery and Kronecker Products. Preprint 58, DFG-SPP 1324, August 2010.

[59] T. Aboiyar, E. H. Georgoulis, and A. Iske. Adaptive ADER Methods Using Kernel-Based Polyharmonic Spline WENO Reconstruction. Preprint 59, DFG-SPP 1324, August 2010.

[60] O. G. Ernst, A. Mugler, H.-J. Starkloff, and E. Ullmann. On the Convergence of Generalized Polynomial Chaos Expansions. Preprint 60, DFG-SPP 1324, August 2010.

[61] S. Holtz, T. Rohwedder, and R. Schneider. On Manifolds of Tensors of Fixed TT-Rank. Preprint 61, DFG-SPP 1324, September 2010.

[62] J. Ballani, L. Grasedyck, and M. Kluge. Black Box Approximation of Tensors in Hierarchical Tucker Format. Preprint 62, DFG-SPP 1324, October 2010.

[63] M. Hansen. On Tensor Products of Quasi-Banach Spaces. Preprint 63, DFG-SPP 1324, October 2010.

[64] S. Dahlke, G. Steidl, and G. Teschke. Shearlet Coorbit Spaces: Compactly Supported Analyzing Shearlets, Traces and Embeddings. Preprint 64, DFG-SPP 1324, October 2010.

[65] W. Hackbusch. Tensorisation of Vectors and their Efficient Convolution. Preprint 65, DFG-SPP 1324, November 2010.

[66] P. A. Cioica, S. Dahlke, S. Kinzel, F. Lindner, T. Raasch, K. Ritter, and R. L. Schilling. Spatial Besov Regularity for Stochastic Partial Differential Equations on Lipschitz Domains. Preprint 66, DFG-SPP 1324, November 2010.

[67] E. Novak and H. Woźniakowski. On the Power of Function Values for the Approximation Problem in Various Settings. Preprint 67, DFG-SPP 1324, November 2010.

[68] A. Hinrichs, E. Novak, and H. Woźniakowski. The Curse of Dimensionality for Monotone and Convex Functions of Many Variables. Preprint 68, DFG-SPP 1324, November 2010.

[69] G. Kutyniok and W.-Q Lim. Image Separation Using Shearlets. Preprint 69, DFG-SPP 1324, November 2010.

[70] B. Jin and P. Maass. An Analysis of Electrical Impedance Tomography with Applications to Tikhonov Regularization. Preprint 70, DFG-SPP 1324, December 2010.

[71] S. Holtz, T. Rohwedder, and R. Schneider. The Alternating Linear Scheme for Tensor Optimisation in the TT Format. Preprint 71, DFG-SPP 1324, December 2010.

[72] T. Müller-Gronbach and K. Ritter. A Local Refinement Strategy for Constructive Quantization of Scalar SDEs. Preprint 72, DFG-SPP 1324, December 2010.

[73] T. Rohwedder and R. Schneider. An Analysis for the DIIS Acceleration Method used in Quantum Chemistry Calculations. Preprint 73, DFG-SPP 1324, December 2010.

[74] C. Bender and J. Steiner. Least-Squares Monte Carlo for Backward SDEs. Preprint 74, DFG-SPP 1324, December 2010.

[75] C. Bender. Primal and Dual Pricing of Multiple Exercise Options in Continuous Time. Preprint 75, DFG-SPP 1324, December 2010.

[76] H. Harbrecht, M. Peters, and R. Schneider. On the Low-rank Approximation by the Pivoted Cholesky Decomposition. Preprint 76, DFG-SPP 1324, December 2010.

[77] P. A. Cioica, S. Dahlke, N. Döhring, S. Kinzel, F. Lindner, T. Raasch, K. Ritter, and R. L. Schilling. Adaptive Wavelet Methods for Elliptic Stochastic Partial Differential Equations. Preprint 77, DFG-SPP 1324, January 2011.

[78] G. Plonka, S. Tenorth, and A. Iske. Optimal Representation of Piecewise Hölder Smooth Bivariate Functions by the Easy Path Wavelet Transform. Preprint 78, DFG-SPP 1324, January 2011.

[79] A. Mugler and H.-J. Starkloff. On Elliptic Partial Differential Equations with Random Coefficients. Preprint 79, DFG-SPP 1324, January 2011.

[80] T. Müller-Gronbach, K. Ritter, and L. Yaroslavtseva. A Derandomization of the Euler Scheme for Scalar Stochastic Differential Equations. Preprint 80, DFG-SPP 1324, January 2011.

[81] W. Dahmen, C. Huang, C. Schwab, and G. Welper. Adaptive Petrov-Galerkin methods for first order transport equations. Preprint 81, DFG-SPP 1324, January 2011.

[82] K. Grella and C. Schwab. Sparse Tensor Spherical Harmonics Approximation in Radiative Transfer. Preprint 82, DFG-SPP 1324, January 2011.

[83] D.A. Lorenz, S. Schiffler, and D. Trede. Beyond Convergence Rates: Exact Inversion With Tikhonov Regularization With Sparsity Constraints. Preprint 83, DFG-SPP 1324, January 2011.

[84] S. Dereich, M. Scheutzow, and R. Schottstedt. Constructive quantization: Approximation by empirical measures. Preprint 84, DFG-SPP 1324, January 2011.

[85] S. Dahlke and W. Sickel. On Besov Regularity of Solutions to Nonlinear Elliptic Partial Differential Equations. Preprint 85, DFG-SPP 1324, January 2011.

[86] S. Dahlke, U. Friedrich, P. Maass, T. Raasch, and R.A. Ressel. An adaptive wavelet method for parameter identification problems in parabolic partial differential equations. Preprint 86, DFG-SPP 1324, January 2011.

[87] A. Cohen, W. Dahmen, and G. Welper. Adaptivity and Variational Stabilization for Convection-Diffusion Equations. Preprint 87, DFG-SPP 1324, January 2011.

[88] T. Jahnke. On Reduced Models for the Chemical Master Equation. Preprint 88, DFG-SPP 1324, January 2011.

[89] P. Binev, W. Dahmen, R. DeVore, P. Lamby, D. Savu, and R. Sharpley. Compressed Sensing and Electron Microscopy. Preprint 89, DFG-SPP 1324, March 2011.

[90] P. Binev, F. Blanco-Silva, D. Blom, W. Dahmen, P. Lamby, R. Sharpley, and T. Vogt. High Quality Image Formation by Nonlocal Means Applied to High-Angle Annular Dark Field Scanning Transmission Electron Microscopy (HAADF-STEM). Preprint 90, DFG-SPP 1324, March 2011.

[91] R. A. Ressel. A Parameter Identification Problem for a Nonlinear Parabolic Differential Equation. Preprint 91, DFG-SPP 1324, May 2011.

[92] G. Kutyniok. Data Separation by Sparse Representations. Preprint 92, DFG-SPP 1324, May 2011.

[93] M. A. Davenport, M. F. Duarte, Y. C. Eldar, and G. Kutyniok. Introduction to Compressed Sensing. Preprint 93, DFG-SPP 1324, May 2011.

[94] H.-C. Kreusler and H. Yserentant. The Mixed Regularity of Electronic Wave Functions in Fractional Order and Weighted Sobolev Spaces. Preprint 94, DFG-SPP 1324, June 2011.

[95] E. Ullmann, H. C. Elman, and O. G. Ernst. Efficient Iterative Solvers for Stochastic Galerkin Discretizations of Log-Transformed Random Diffusion Problems. Preprint 95, DFG-SPP 1324, June 2011.

[96] S. Kunis and I. Melzer. On the Butterfly Sparse Fourier Transform. Preprint 96, DFG-SPP 1324, June 2011.

[97] T. Rohwedder. The Continuous Coupled Cluster Formulation for the Electronic Schrödinger Equation. Preprint 97, DFG-SPP 1324, June 2011.

[98] T. Rohwedder and R. Schneider. Error Estimates for the Coupled Cluster Method. Preprint 98, DFG-SPP 1324, June 2011.

[99] P. A. Cioica and S. Dahlke. Spatial Besov Regularity for Semilinear Stochastic Partial Differential Equations on Bounded Lipschitz Domains. Preprint 99, DFG-SPP 1324, July 2011.

[100] L. Grasedyck and W. Hackbusch. An Introduction to Hierarchical (H-) Rank and TT-Rank of Tensors with Examples. Preprint 100, DFG-SPP 1324, August 2011.

[101] N. Chegini, S. Dahlke, U. Friedrich, and R. Stevenson. Piecewise Tensor Product Wavelet Bases by Extensions and Approximation Rates. Preprint 101, DFG-SPP 1324, September 2011.

[102] S. Dahlke, P. Oswald, and T. Raasch. A Note on Quarkonial Systems and Multilevel Partition of Unity Methods. Preprint 102, DFG-SPP 1324, September 2011.

[103] A. Uschmajew. Local Convergence of the Alternating Least Squares Algorithm For Canonical Tensor Approximation. Preprint 103, DFG-SPP 1324, September 2011.

[104] S. Kvaal. Multiconfigurational time-dependent Hartree method for describing particle loss due to absorbing boundary conditions. Preprint 104, DFG-SPP 1324, September 2011.

[105] M. Guillemard and A. Iske. On Groupoid C*-Algebras, Persistent Homology and Time-Frequency Analysis. Preprint 105, DFG-SPP 1324, September 2011.

[106] A. Hinrichs, E. Novak, and H. Woźniakowski. Discontinuous information in the worst case and randomized settings. Preprint 106, DFG-SPP 1324, September 2011.

[107] M. Espig, W. Hackbusch, A. Litvinenko, H. Matthies, and E. Zander. Efficient Analysis of High Dimensional Data in Tensor Formats. Preprint 107, DFG-SPP 1324, September 2011.

[108] M. Espig, W. Hackbusch, S. Handschuh, and R. Schneider. Optimization Problems in Contracted Tensor Networks. Preprint 108, DFG-SPP 1324, October 2011.

[109] S. Dereich, T. Müller-Gronbach, and K. Ritter. On the Complexity of Computing Quadrature Formulas for SDEs. Preprint 109, DFG-SPP 1324, October 2011.

[110] D. Belomestny. Solving optimal stopping problems by empirical dual optimization and penalization. Preprint 110, DFG-SPP 1324, November 2011.

[111] D. Belomestny and J. Schoenmakers. Multilevel dual approach for pricing American style derivatives. Preprint 111, DFG-SPP 1324, November 2011.

[112] T. Rohwedder and A. Uschmajew. Local convergence of alternating schemes for optimization of convex problems in the TT format. Preprint 112, DFG-SPP 1324, December 2011.

[113] T. Görner, R. Hielscher, and S. Kunis. Efficient and accurate computation of spherical mean values at scattered center points. Preprint 113, DFG-SPP 1324, December 2011.

[114] Y. Dong, T. Görner, and S. Kunis. An iterative reconstruction scheme for photoacoustic imaging. Preprint 114, DFG-SPP 1324, December 2011.

[115] L. Kämmerer. Reconstructing hyperbolic cross trigonometric polynomials by sampling along generated sets. Preprint 115, DFG-SPP 1324, February 2012.

[116] H. Chen and R. Schneider. Numerical analysis of augmented plane waves methods for full-potential electronic structure calculations. Preprint 116, DFG-SPP 1324, February 2012.

[117] J. Ma, G. Plonka, and M.Y. Hussaini. Compressive Video Sampling with Approximate Message Passing Decoding. Preprint 117, DFG-SPP 1324, February 2012.

[118] D. Heinen and G. Plonka. Wavelet shrinkage on paths for scattered data denoising. Preprint 118, DFG-SPP 1324, February 2012.